Optimisation of the Shape of the Ferromagnetic Core of Fluxset Type Magnetic Field Sensors

József Pávó
Department of Electromagnetic Theory, Technical University of Budapest, Egry József u. 18. H-1521 Budapest, Hungary

Abstract–**A method is presented for the optimisation of the shape of the ferromagnetic core of fluxset type magnetic filed sensors. The objective of the optimisation is to find a core shape that guarantees the most homogeneous magnetisation of the core due to a given external magnetic field. By finding the optimal shape of the core the sensitivity of the sensor is improved. Since the thickness of the ferromagnetic conducting ribbon core used for fluxset sensors is considerably smaller than its other dimensions, the presence of the core is modelled by magnetic and conducting surface currents flowing in a mathematical surface representing the core. The electromagnetic field is calculated by solving an integral equation derived from the assumption of impedance type boundary conditions on the two sides of this surface. The core shape is optimised by minimising the magnetisation differences at different locations of the core. Simulated annealing procedure is used for the optimisation.**

I. Introduction

Fluxset type magnetic field sensors are used for the measurement of weak magnetic fields in various applications, such as geomagnetic measurements or eddy current testing (ECT) [1], [2]. The basic components of a fluxset sensor are an exciting solenoid and a pick-up solenoid wound around a ribbon shape ferromagnetic core (see Fig. 1). The magnetisation of the core due to the magnetic field generated by the exciting solenoid can be changed by varying the shape of the core. The more homogeneous the magnetisation of the core material, the better the sensitivity of the sensor. In this paper an optimisation method is presented that can be used for finding the optimal core shape for a given exciting field.

To find the optimal shape, the solution of the related direct problem, i.e. the calculation of the magnetisation of a given core due to an external magnetic field, is required. Since the thickness of the core is negligible compared to its other dimensions, it is advantageous to assume it as a mathematical surface. The presence of the ferromagnetic core is modelled by magnetic and conducting surface currents flowing in the surface representing the core. The actual distribution of the surface currents is calculated by solving an integral equation derived from the enforcement of the impedance type boundary conditions [3], [4] on the two sides of the core surface. The numerical solution of the integral equation is calculated by using analytical expressions for the spatial Fourier transform (FT) of the elements of the dyadic Green's functions related to the magnetic and conducting surface currents.

Manuscript received October 8, 1996
J. Pávó, e-mail pavo@evtsz1.evt.bme.hu, fax +36 1 463-3189

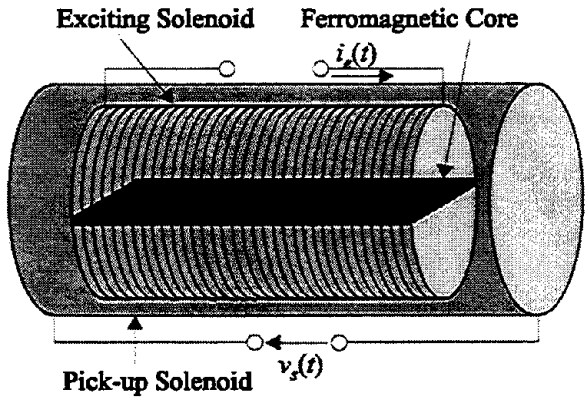

Fig. 1. Schematic drawing of a fluxset sensor.

On the basis of the above outlined solution of the direct problem, the optimisation of the core shape is made by using simulated annealing optimisation procedure. The objective of the optimisation is the minimisation of the deviation of the magnetisation at different spots on the surface of the core from the average value of the magnetisation. Several constraints dictated by technological reasons are also posed on the optimisation procedure.

In the followings first the operation principle of the fluxset sensor is outlined to explain the objectives of the shape optimisation. After this, the derivation and numerical solution of the integral equation used for the modelling of the ferromagnetic conductor core is discussed. Finally the procedure used for finding the optimal shape of the core is explained. Several numerical and experimental examples are also presented to demonstrate the results of the paper.

II. Operation Principle of Fluxset Sensors

The schematic drawing of a fluxset sensor is shown in Fig. 1. The sensor is made of two solenoids wound on each other. The inner and outer solenoids are called exciting solenoid and pick-up solenoid, respectively. In the middle of the sensor the ribbon shape core is located. The core is an annealed metallic glass that is a very good soft magnetic material with high initial permeability and low saturation.

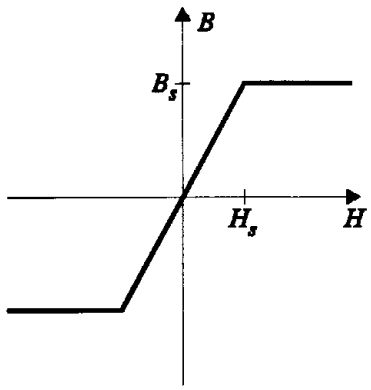

Fig. 2. Idealised *BH* curve of the core material.

The idealised *BH* curve of the core material is shown in Fig. 2. The initial relative permeability and conductivity of the core are about μ_r=85,000 and σ=1.0 10^5 S/m, respectively, the material saturates on about B_s=1 T. The actual *BH* curve and other parameters of the material are strongly depend on the different mechanical, heat, chemical, etc. treatments of the raw material carried out to improve the magnetic properties of the core. The approximate length and diameter of the sensor are 8 mm and 2 mm, respectively. The thickness of the ribbon core is 40 μm.

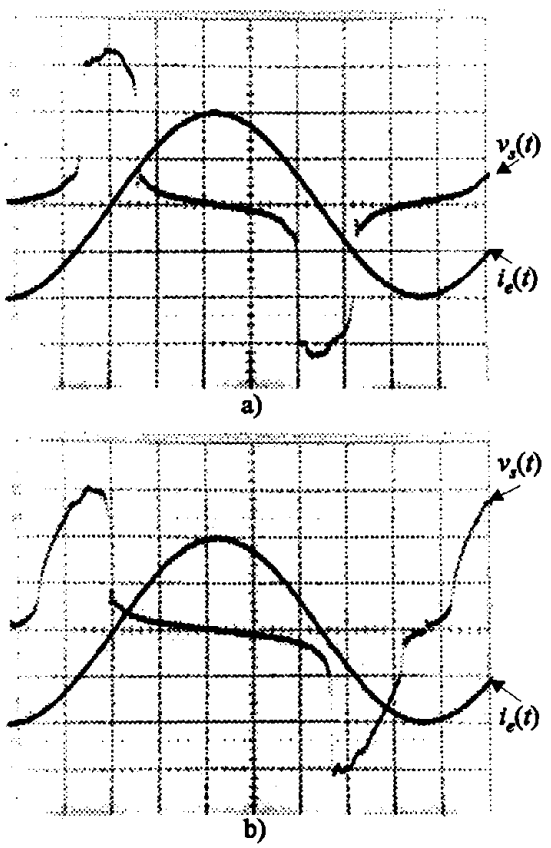

Fig. 3. Oscilloscope plot of the current of the exciting solenoid, $i_e(t)$, and the voltage of the pick-up solenoid, $v_s(t)$. a) without external magnetic field, b) with external magnetic field.

In Fig. 3 the oscilloscope plot of the current of the exciting coil, $i_e(t)$, and the voltage of the pick-up coil, $v_s(t)$, are shown. Considering the idealised magnetisation curve shown in Fig. 2, we can see in Fig. 3.a that the induced voltage in the pick-up solenoid, $v_s(t)$, is almost zero when the core is saturated, on the other hand this induced voltage is a relatively large value (proportional to the time derivative of the exciting current) while the exciting magnetic field changes its direction (i.e. the core material is magnetised in the linear range). If an external magnetic field (i.e. the field to be measured) is superimposed on the periodic excitation, the time spent in saturation in one direction (e.g. when $B=B_s$) is longer than the time spent in saturation in the other direction (e.g. when $B=-B_s$), as a result the impulse, $v_s(t)$, is shifted. This situation is shown in Fig. 3.b. The time shift of the impulse, $v_s(t)$, can be accurately measured, consequently the external field can be predicted.

The accuracy of the measurement basically depends on the shape of the pulse, $v_s(t)$, detected on the sensor coil. It can be seen that, the sharper the detected voltage signal, the easier to detect small time differences, consequently the magnetic field is measured more accurately. On the basis of this consideration we may conclude that the more uniform the magnetic field in the core (i.e. the different regions of the core are saturated in the same time instant), the higher accuracy can be achieved in the measurement. The requirement of the uniformity of the magnetic field in the core might be fulfilled by changing the shape of the sensor core. Since the pulse shape is formed by the fast change of the magnetic flux density inside the core when the exciting field changes its sign, the time dependence of the pulse can be calculated by assuming a linear ferromagnetic material that permeability is obtained as the gradient of the linear part of the *BH* curve. Of course, the results of such calculations are useful only if the core material is not saturated. Since our goal is to find a configuration where the whole volume of the sensor core is saturated in the same time instant, the assumption of linear ferromagnetic material is acceptable.

III. Calculation of the Magnetisation of the Core

A. The Integral Equation

Assume that a linear ferromagnetic conductor film is placed in the z=0 plane of a Cartesian co-ordinate system (see Fig. 4). The conductivity, permeability and thickness of the film are μ_1, σ_1 and h, respectively. The electromagnetic field is assumed to vary in time as the real part of $\exp(j\omega t)$ where ω is the angular frequency of the excitation. Since the thickness of the film is considerably smaller than its other dimensions, the film is modelled as a mathematical surface, S, having zero thickness. The behaviours of the tangential component of the electric and magnetic fields on the two sides of surface, S, are approximated as they were on the two sides of an infinite plate that thickness is h. This behaviour is

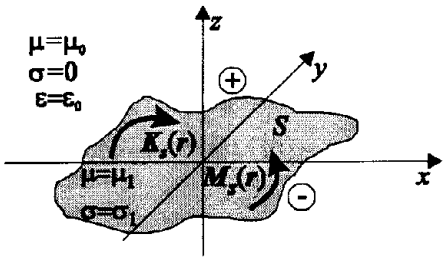

Fig. 4. Ferromagnetic conductor film in the z=0 plane.

expressed by the so called impedance type boundary conditions [3], [4],

$$\boldsymbol{H}_t^+ - \boldsymbol{H}_t^- = \frac{\sigma_1}{\eta}\tanh\left(\frac{\eta h}{2}\right)\hat{n}\times\left(\boldsymbol{E}_t^+ + \boldsymbol{E}_t^-\right), \tag{1}$$

$$\boldsymbol{E}_t^+ - \boldsymbol{E}_t^- = \frac{\eta}{\sigma_1}\tanh\left(\frac{\eta h}{2}\right)\hat{n}\times\left(\boldsymbol{H}_t^+ + \boldsymbol{H}_t^-\right), \tag{2}$$

where $\eta = \sqrt{j\omega\sigma_1\mu_1}$, $\boldsymbol{E}_t$ and $\boldsymbol{H}_t$ denote the tangential components of the electric and magnetic fields on the surface, S. Subscripts + and – refer to the filed values on the z=+0 and z=–0 sides of the surface. $\hat{n}$ is the normal vector of surface, S.

The jump in the tangential electric and magnetic fields prescribed by (1) and (2) might be realised by placing the magnetic surface current, $\boldsymbol{M}_s(\boldsymbol{r})$, and the conducting surface current, $\boldsymbol{K}_s(\boldsymbol{r})$, as secondary sources in the surface, S ($\boldsymbol{r}$ denotes the spatial co-ordinate vector). Based on the outlined model the electric field, $\boldsymbol{E}$, and the magnetic field, $\boldsymbol{H}$, in the presence of the ferromagnetic film can be obtained as,

$$\boldsymbol{H} = \boldsymbol{H}_0 + \boldsymbol{H}_f, \tag{3}$$

$$\boldsymbol{E} = \boldsymbol{E}_0 + \boldsymbol{E}_f, \tag{4}$$

where the subscript 0 refers the external field (in the case of the fluxset sensor this external field is the one that is generated by the exciting solenoid). The field quantities with the subscript f denote the electromagnetic field generated by the secondary sources, $\boldsymbol{M}_s(\boldsymbol{r})$ and $\boldsymbol{K}_s(\boldsymbol{r})$, representing the presence of the ferromagnetic film. $\boldsymbol{H}_f$ and $\boldsymbol{E}_f$ can be expressed with the help of dyadic Green's functions in the following form:

$$\boldsymbol{E}_f = \int_S \left[\nabla\times\mathbf{G}(\boldsymbol{r}|\boldsymbol{r}')\cdot\boldsymbol{M}_s(\boldsymbol{r}') - j\omega\mu_0\mathbf{G}(\boldsymbol{r}|\boldsymbol{r}')\cdot\boldsymbol{K}_s(\boldsymbol{r}')\right]ds', \tag{5}$$

$$\boldsymbol{H}_f = \int_S \left[j\omega\varepsilon_0\mathbf{G}(\boldsymbol{r}|\boldsymbol{r}')\cdot\boldsymbol{M}_s(\boldsymbol{r}') + \nabla\times\mathbf{G}(\boldsymbol{r}|\boldsymbol{r}')\cdot\boldsymbol{K}_s(\boldsymbol{r}')\right]ds', \tag{6}$$

where ε_0 and μ_0 are the permittivity and permeability of the free space, respectively. $\mathbf{G}(\boldsymbol{r}|\boldsymbol{r}')$ is the dyadic Green's function transforming the excitation into the field components. $\boldsymbol{r}$ and $\boldsymbol{r}'$ are the co-ordinates of the field and the source points, respectively. $\mathbf{G}(\boldsymbol{r}|\boldsymbol{r}')$ is obtained by the solution of the equation [5],

$$\nabla\times\nabla\times\mathbf{G}(\boldsymbol{r}|\boldsymbol{r}') - \omega^2\mu_0\varepsilon_0\mathbf{G}(\boldsymbol{r}|\boldsymbol{r}') = \delta(\boldsymbol{r}-\boldsymbol{r}')\mathbf{I}, \tag{7}$$

where $\mathbf{I}$ is the unit dyad defined as,

$$\mathbf{I} = \hat{x}\hat{x} + \hat{y}\hat{y} + \hat{z}\hat{z}, \tag{8}$$

and $\hat{x}$, $\hat{y}$ and $\hat{z}$ denote the unit vectors of the co-ordinate system.

Having the expressions (5) and (6) with the assumption that the external field is continuous on the surface, S, the following integral equations are obtained for the unknown secondary sources, $\boldsymbol{M}_s(\boldsymbol{r})$ and $\boldsymbol{K}_s(\boldsymbol{r})$, modelling the effect of the presence of the ferromagnetic film:

$$\frac{\eta}{\sigma_1}\coth\left(\frac{\eta h}{2}\right)\left(\boldsymbol{H}_{ft}^+ - \boldsymbol{H}_{ft}^-\right) - \hat{n}\times\left(\boldsymbol{E}_{ft}^+ + \boldsymbol{E}_{ft}^-\right) = 2\hat{n}\times\boldsymbol{E}_{0t}, \tag{9}$$

$$\frac{\sigma_1}{\eta}\coth\left(\frac{\eta h}{2}\right)\left(\boldsymbol{E}_{ft}^+ - \boldsymbol{E}_{ft}^-\right) - \hat{n}\times\left(\boldsymbol{H}_{ft}^+ + \boldsymbol{H}_{ft}^-\right) = 2\hat{n}\times\boldsymbol{H}_{0t}, \tag{10}$$

where superscripts +, – and subscripts 0, t, f have the same meaning like in (1)-(4).

For special geometrical arrangements the above integral equation might be simplified. Such situation is when the ferromagnetic film is placed in free space. In this case only the magnetic surface currents are needed for the calculation of the tangential magnetic field on the surface, S. This special case will be applied for the optimisation of the core of the fluxset sensor.

B. Numerical Solution of the Integral Equation

Considering the arrangement and co-ordinate system shown in Fig. 3, the discrete approximation of integral equations (9), (10) is found by approximating the unknown functions, $\boldsymbol{M}_s(\boldsymbol{r})$ and $\boldsymbol{K}_s(\boldsymbol{r})$, as,

$$\boldsymbol{M}_s(x,y) \approx \sum_{n=1}^{N}\boldsymbol{M}_s^n a_n(x,y) = \sum_{n=1}^{N}\left(M_{sx}^n\hat{x} + M_{sy}^n\hat{y}\right)a_n(x,y); \quad x,y\in S \tag{11}$$

$$\boldsymbol{K}_s(x,y) \approx \sum_{n=1}^{N}\boldsymbol{K}_s^n a_n(x,y) = \sum_{n=1}^{N}\left(K_{sx}^n\hat{x} + K_{sy}^n\hat{y}\right)a_n(x,y); \quad x,y\in S \tag{12}$$

where $a_n(x,y)$ denotes the approximating function. Although the method outlined here is easily applicable for rather wide class of approximating functions, the computer code

developed for the optimisation of the sensor core uses linear approximating functions. Accordingly, the surface, S, is subdivided into a regular grid of N cells, each cell being a rectangle, the co-ordinates of the n-th grid point are $(x_n;y_n)$. The distances between the nearby points in the x and y co-ordinate directions are Δx and Δy, respectively. Consequently the approximating functions are,

$$a_n(x,y)=f\left(\frac{x-x_n}{\Delta x},\frac{y-y_n}{\Delta y}\right), \qquad n=1,2,\ldots,N;$$
$$f(x,y)=\begin{cases}1-|x|-|y|+|xy|, & -1<x,y<1;\\ 0, & \text{otherwise;}\end{cases} \tag{13}$$

In the followings we will use the two-dimensional spatial Fourier transform (FT) of spatial functions. In the case of the approximating function the FT is denoted and defined as,

$$\tilde{a}_n(\alpha,\beta)=\tilde{F}\{a_n(x,y)\}=\int_{-\infty}^{\infty}\int_{-\infty}^{\infty}a_n(x,y)e^{j(\alpha x+\beta y)}\,dxdy, \tag{14}$$

where α and β are the pairs of the x and y co-ordinates in the Fourier transform plane.

Using similar considerations presented in [6], the FT of the electric and magnetic field generated by the approximation of the surface currents (11) and (12) can be expressed analytically in the following form (superscripts + and – refer to the field in the $z>0$ and $z<0$ half spaces, respectively),

$$\tilde{H}_{fx}^{\pm}(\alpha,\beta,z)=\tilde{F}\{\boldsymbol{H}_f^{\pm}(x,y,z)\cdot\hat{x}\}=$$
$$=\sum_{n=1}^{N}\left[\frac{(\beta^2+\gamma^2)M_{sx}^n-\alpha\beta M_{sy}^n}{2\omega\mu_0\gamma}\pm\frac{K_{sy}^n}{2}\right]\tilde{a}_n(\alpha,\beta)e^{-j\gamma|z|}, \tag{15}$$

$$\tilde{H}_{fy}^{\pm}(\alpha,\beta,z)=\tilde{F}\{\boldsymbol{H}_f^{\pm}(x,y,z)\cdot\hat{y}\}=$$
$$=\sum_{n=1}^{N}\left[\frac{-\alpha\beta M_{sx}^n+(\alpha^2+\gamma^2)M_{sy}^n}{2\omega\mu_0\gamma}\mp\frac{K_{sx}^n}{2}\right]\tilde{a}_n(\alpha,\beta)e^{-j\gamma|z|}, \tag{16}$$

$$\tilde{H}_{fz}^{\pm}(\alpha,\beta,z)=\tilde{F}\{\boldsymbol{H}_f^{\pm}(x,y,z)\cdot\hat{z}\}=$$
$$=\sum_{n=1}^{N}\left[\mp\frac{\alpha M_{sx}^n+\beta M_{sy}^n}{2\omega\mu_0}\pm\frac{\beta K_{sx}^n-\alpha K_{sy}^n}{2\gamma}\right]\tilde{a}_n(\alpha,\beta)e^{-j\gamma|z|}, \tag{17}$$

$$\tilde{E}_{fx}^{\pm}(\alpha,\beta,z)=\tilde{F}\{\boldsymbol{E}_f^{\pm}(x,y,z)\cdot\hat{x}\}=$$
$$=\sum_{n=1}^{N}\left[\frac{-(\beta^2+\gamma^2)K_{sx}^n+\alpha\beta K_{sy}^n}{2\omega\varepsilon_0\gamma}\pm\frac{M_{sy}^n}{2}\right]\tilde{a}_n(\alpha,\beta)e^{-j\gamma|z|}, \tag{18}$$

$$\tilde{E}_{fy}^{\pm}(\alpha,\beta,z)=\tilde{F}\{\boldsymbol{E}_f^{\pm}(x,y,z)\cdot\hat{y}\}=$$
$$=\sum_{n=1}^{N}\left[\frac{\alpha\beta K_{sx}^n-(\alpha^2+\gamma^2)K_{sy}^n}{2\omega\varepsilon_0\gamma}\mp\frac{M_{sx}^n}{2}\right]\tilde{a}_n(\alpha,\beta)e^{-j\gamma|z|}, \tag{19}$$

$$\tilde{E}_{fz}^{\pm}(\alpha,\beta,z)=\tilde{F}\{\boldsymbol{E}_f^{\pm}(x,y,z)\cdot\hat{z}\}=$$
$$=\sum_{n=1}^{N}\left[\pm\frac{\alpha K_{sx}^n+\beta K_{sy}^n}{2\omega\varepsilon_0}\pm\frac{\beta M_{sx}^n-\alpha M_{sy}^n}{2\gamma}\right]\tilde{a}_n(\alpha,\beta)e^{-j\gamma|z|}, \tag{20}$$

where,

$$\gamma=\begin{cases}\sqrt{\omega^2\mu_0\varepsilon_0-\alpha^2-\beta^2}, & \omega^2\mu_0\varepsilon_0>\alpha^2+\beta^2;\\ -j\sqrt{\alpha^2+\beta^2-\omega^2\mu_0\varepsilon_0}, & \omega^2\mu_0\varepsilon_0<\alpha^2+\beta^2;\end{cases} \tag{21}$$

Having a look at the above expressions, we can see that they can be applied for the kind of approximations where the FT of the approximating functions, $a_n(x,y)$ (n=1, 2, ...,N), exist. Practically most of the possible approximations meet this requirement.

Taking the inverse FT of the expressions, (15)-(20), and testing them with the testing functions, $t_m(x,y)$ (m=1,2,...,N), a system of $4N$ linear equations is obtained for the $4N$ unknown coefficients, M_{sx}^n, M_{sy}^n, K_{sx}^n, K_{sy}^n (n=1,2,...,N). In the numerical examples presented in this paper, linear testing functions are used, i.e.,

$$t_m(x,y)=f\left(\frac{x-x_m}{\Delta x},\frac{y-y_m}{\Delta y}\right), \qquad m=1,2,\ldots,N; \tag{22}$$

After solving the obtained equation system, the electromagnetic field can be evaluated using (3), (4) and (15)-(20), consequently the magnetic field can be calculated on the two sides of surface, S. Based on the well-known interface conditions (continuity of the tangential component of the magnetic field and the normal component of the magnetic flux density at the interface of the film and air), the magnetisation of the ferromagnetic film can be also evaluated. Since the relative permeability of the ferromagnetic material used for the core of the fluxset sensor is very high (μ_r=85,000), our design requirement will be the smoothness of the amplitude of the tangential component of the magnetic field on the surface, S.

C. Numerical Example

A computer code has been developed for the above described numerical calculations. As an example, the tangential magnetic field on the surface of an elliptical shape core is calculated. The principle axis of the ellipsis is 5 mm and it is parallel to the x axis, the minor axis of it is 0.8 mm. The relative permeability and conductivity of the film are μ_r=85,000 and σ=1.0 10^5 S/m, respectively. The frequency of the excitation is f=10.0 kHz. The ferromagnetic film is placed in the homogeneous x-directed external magnetic field that amplitude is 1.0 A/m.

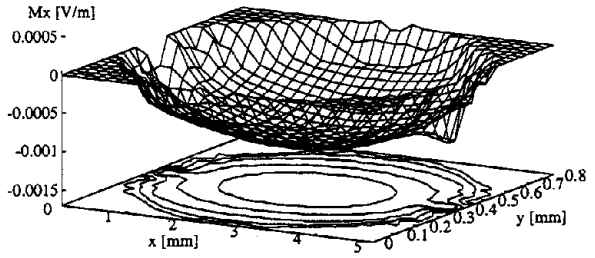

Fig. 5. x component of the magnetic surface current density representing the ferromagnetic film (out of phase with the external magnetic field).

In Fig. 5 the x component of the magnetic surface current modelling the presence of the ferromagnetic film is plotted. (Note that in the following plots the function values corresponding to the points outside of the film surface are set to zero, these values have no meaning.) The y component of the magnetic surface current is considerably smaller than its x component, this is because of the particular excitation and because of the dimensions of the ellipsis (the principle axis is 6.25 times bigger than the minor axis). Figure 6 shows the x component of the magnetic field on the surface of the film. The y component of the magnetic field - due to similar reasons mentioned before - is negligible, consequently the magnetisation of the film can be characterised almost entirely with the values plotted in Fig. 6. The ratio of the in

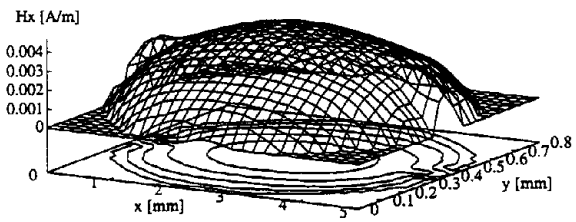

a)

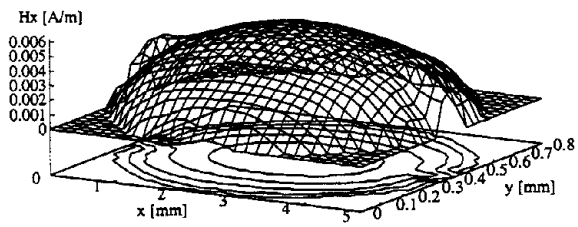

b)

Fig. 6. x component of the magnetic field on the surface of the ferromagnetic film. a) in phase with the external magnetic field, b) out of phase with the external magnetic field.

phase and out of phase components gives information on the phase shift of the sensor signal with respect to the external field.

IV. Optimisation of the Core Shape

Based on the outlined method for the calculation of the magnetisation of the sensor core, the optimal core shape is found by simulated annealing optimisation procedure. The objective, expressing the requirement of smoothness of the magnetisation of the core material, is the minimisation of the expression,

$$\frac{\sum_{n=1}^{N}\left|\overline{H}_t - H_t^n\right|}{N} \tag{23}$$

where $\overline{H}_t$ denotes the average of the absolute value of the tangential magnetic field on the surface, S, and H_t^n is the absolute value of the tangential component of the magnetic field at the n-th grid point. This objective function gives the value of 35.1% for the elliptical shape core analysed in the previous section.

Several constraints are posed on the optimisation. One of the constraints comes from the symmetry of the sensor arrangement, consequently the core is designed to be also symmetric. By the outer dimension of the sensor, the maximum size of the core is defined, it cannot be bigger than a 5mm×0.8mm rectangle (see Fig. 7). To obtain a sensor signal with sufficient amplitude, the minimal size of the core is also fixed (see white area in Fig. 7). In Fig. 7 the shapes corresponding to the first and final approximations of the optimisation, i.e. the initial and the final shapes, are also shown.

Due to the symmetry and the special elongated shape of the sensor, the shape of the core is described with a small number of parameters, accordingly, the number of degrees of freedom of the optimisation is 4. The particular choice of the simulated annealing optimisation procedure [7] is supported by the facts that it is very easy to apply this algorithm and it works almost for sure if it is properly implemented. On the other hand, the efficiency of this method is not particularly good because of the high number of function calls required for finding the optimum. However, the design of a fluxset sensor is not a kind of problem that has to be solved very frequently, that is why the robustness of the optimisation is the primary concern and the efficiency is not crucially important.

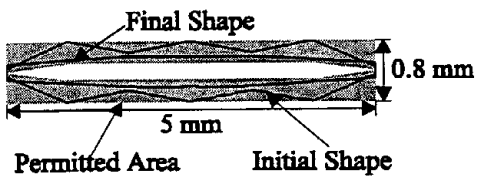

Fig. 7 Constraints of the optimisation and the initial and final shapes.

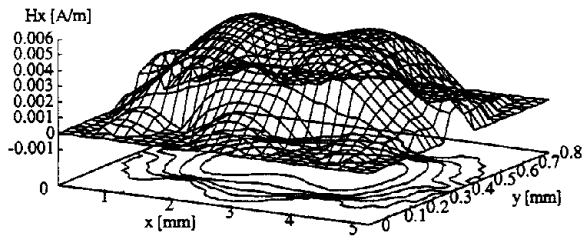

a)

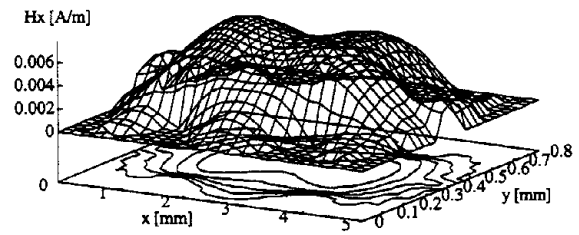

b)

Fig. 8. x component of the tangential magnetic field for the initial shape core. a) in phase with the external magnetic field, b) out of phase with the external magnetic field.

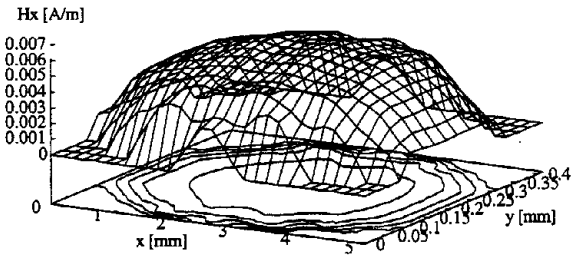

a)

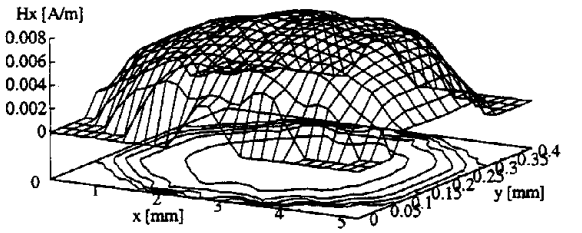

b)

Fig. 9. x component of the tangential magnetic field for the optimum shape core. a) in phase with the external magnetic field, b) out of phase with the external magnetic field.

In Fig. 8 the x component of the tangential magnetic field in the case of the initial shape is plotted. In Fig. 9 the tangential magnetic field of the optimal shape sensor core is shown. The objective function, (23), for the initial and final shapes are 54.4% and 29.5%, respectively.

CONCLUSIONS

An optimisation method has been presented for the design of the ferromagnetic core of fluxset sensors. As the part of the method, the solution of the related direct problem, i.e. the calculation of the magnetisation of a ferromagnetic conductor thin film due to a given external field, has been discussed. The presence of the ferromagnetic conductor film has been represented by magnetic and conducting surface currents. The actual distribution of these surface currents has been obtained by the numerical solution of an integral equation derived from the application of the impedance type boundary conditions at the surface representing the film. The integral equation has been solved by using analytical expressions for the spatial Fourier transform of the electromagnetic field generated by the surface currents representing the ferromagnetic film. On the basis of the solution of the direct problem, the shape of a fluxset sensor has been optimised by using simulated annealing procedure. Numerical examples have been presented for the demonstration of the results of the paper.

ACKNOWLEDGMENT

The author would like to thank Antal Gasparics of Department of Electromagnetic Theory, Technical University of Budapest, Hungary, for the preparation and recording of the presented oscilloscope plots.

REFERENCES

[1] G. Vertesy, J. Szollosy, K.L. Varga and A. Lovas, "High sensitivity magnetic field sensor using amorphous alloy," *Electronic Horizon*, vol.53, p.102, 1992.

[2] Cs.S. Daróczi et al., "Electromagnetic NDT material testing," in *Nondestructive Testing of Materials*, eds.: R. Collins, W.D. Dover, J.R. Bowler and K. Miya, IOS Press, Amsterdam, pp.75-86, 1995.

[3] L. Krähenbühl and D. Muller, "Thin layers in electric engineering. Example of shell models in analysing eddy-currents by boundary and finite element methods," *IEEE Transaction on Magnetics*, vol. 29, No. 2, pp.1450-1455, March 1993.

[4] I.D. Mayergoyz and G. Bedrosian, "On calculation of 3-D eddy currents in conducting and magnetic shells," *IEEE Transaction on Magnetics*, vol. 31, No. 3, pp.1319-1324, May 1995.

[5] C.T. Tai, *Dyadic Green's Functions in Electromagnetic Theory*, Scranton, Pennsylvania, USA: Intext, 1971.

[6] J. Pavo and K. Miya, "Reconstruction of crack shape by optimization using eddy current field measurement," *IEEE Transaction on Magnetics*, vol. 30, pp.3407-3410, September 1994.

[7] W. H. Press et al., *Numerical Recipes*, Cambridge: Cambridge University Press, 1986.